JOURNAL OF Materials CHEMISTRY

Hydrothermal synthesis and *ab initio* structural approach of two new layered oxyfluorinated titanium(IV) phosphates: $Ti_2(PO_4)_2F_4{\cdot}N_2C_2H_{10}$ (MIL-6) and $Ti_2(PO_4)_2F_4{\cdot}N_2C_3H_{12}{\cdot}H_2O$

Christian Serre and Gérard Férey*

Institut Lavoisier, UMR CNRS 173, 45 Avenue des Etats-Unis 78035 Versailles Cedex, France.
E-mail: serre@chimie.uvsq.fr; ferey@chimie.uvsq.fr

Received 9th April 1998, Accepted 26th October 1998

$Ti_2(PO_4)_2F_4{\cdot}N_2C_2H_{10}$ (MIL-6) and $Ti_2(PO_4)_2F_4{\cdot}N_2C_3H_{12}{\cdot}H_2O$ were prepared hydrothermally (3 days, 453–483 K, autogenous pressure) in the presence of an organic template (ethylenediamine or 1,3-diaminopropane). The structures of $Ti_2(PO_4)_2F_4{\cdot}N_2C_2H_{10}$ **1** and $Ti_2(PO_4)_2F_4{\cdot}N_2C_3H_{12}{\cdot}H_2O$ **2** were determined *ab initio* from powder diffraction data. These structures exhibit different monoclinic distortions of the $VOPO_4{\cdot}2H_2O$ structure type. **1**: space group $P2_1/c$ (no. 14), $a=7.508(1)$, $b=8.881(1)$, $c=8.961(1)$ Å, $\beta=107.22(1)°$ and $V=570.8(1)$ Å^3. **2**: space group $C2$ (no. 5), $a=16.820(2)$, $b=6.333(2)$, $c=6.331(2)$ Å, $\beta=106.20°$ and $V=645.8(1)$ Å^3. Both are layered compounds built up from TiO_4F_2 octahedra linked together by PO_4 tetrahedra; the Ti–F bonds are oriented perpendicularly to the layers which contain the diprotonated amine. The stability of the structures is ensured by the strong hydrogen bonding between the fluorine atoms and the amino groups.

1 Introduction

Since 1992, our group has been characterising a series of oxyfluorinated metallophosphates (denoted ULM-*n*).[1,2] From the study of the relation between chemical parameters and the structure of alumino- and gallo-phosphates, a hypothesis for the mechanism of formation of these compounds was proposed, which suggested that the syntheses of metallophosphates with M = 3d transition element were possible.[1] Several oxyfluorinated solids containing vanadium or iron as the metal were then discovered; the vanadium compounds are layered solids,[3,4] except for ULM-7 which is the first framework with a microporous structure described so far with this cation.[5] Most of the iron family compounds are three-dimensional and exhibit interesting antiferromagnetic properties in the temperature range 10–37 K (ULM-3, ULM-4, ULM-12, ULM-15 and 19).[6–10] While the number of porous solids containing trivalent ions is increasing sharply, there are only few results concerning tetravalent elements.

For the titanium phosphate family of compounds, very few phases have been reported up to now: the well known α-TiP and γ-TiP synthesised in the 1960–70s,[11,12] the three-dimensional KTP ($KTiOPO_4$),[13] and the $MTi_2(PO_4)_3$ compounds (M = Li, Na ...).[14,15] Recently, three other layered titanium phosphates of formulae $TiO(OH)(H_2PO_4){\cdot}2H_2O$,[16] $Ti_2O_3(H_2PO_4){\cdot}2H_2O$,[17] and β-$Ti(PO_4)(H_2PO_4)$, an anhydrous form of the γ-TiP,[18] have been characterised. The only microporous titanium phosphate compounds characterised up to now have been synthesised by Clearfield and coworkers,[19] but no oxyfluorinated titanium phosphates have been characterised to date. However, two oxyfluorinated zirconium phosphate compounds have been structurally determined recently: one of them is a layered compound,[20] while the second exhibits a three dimensional structure with an open framework.[21]

Our group has undertaken a systematic study of the titanium system, and this paper presents the first results relating to the synthesis and the *ab initio* structural determination of the first two layered oxyfluorinated titanium phosphates; $Ti_2(PO_4)_2F_4{\cdot}N_2C_2H_{10}$ **1** and $Ti_2(PO_4)_2F_4{\cdot}N_2C_3H_{12}{\cdot}H_2O$ **2**. However, very strong orientation effects were observed and prevented an accurate structure determination. Therefore, only the synthesis, compositions and crude structure determination, as stated in the title, are reported.

2 Experimental

2.1 Synthesis and analysis

Hydrous titanium dioxide was prepared from the reaction of strongly acidic solutions of $TiCl_4$ (Aldrich, 99%) in HCl (Prolabo, 36%) with ammonia (Prolabo, 20%) at room temperature; the precipitate was washed with demineralised water and dried at 373 K.

Compound **1** was hydrothermally synthesised from hydrous TiO_2, H_3PO_4 (Prolabo Normapur 85%), HF (Prolabo Normapur 40%), ethylenediamine (Aldrich 97%) and H_2O in the molar ratio 1 : 1 : 4 : 0.5 : 80. For compound **2**, the diamine was 1,3-diaminopropane (Aldrich, 99%) and the molar ratio 1 : 1 : 5 : 0.5 : 80. The mixtures were placed without stirring in a Teflon-lined steel autoclave under autogenous pressure for 3 days at 483 K for **1** and 453 K for **2**. The resulting white products were washed with demineralised water and dried at room temperature.

The TGA experiments, performed with a Texas Instrument OAos apparatus under oxygen flow, showed weight losses between 473 and 673 K of 18 and 20% for **1** and **2** respectively; these results were in relatively good agreement with the theoretical calculations for the loss of the organic template (% theoretical loss = 15% for **1** and 18% for **2**). For compound **2**, the TGA also showed another weight loss of 3.3% between 323 and 373 K corresponding to the departure of the water; this result agreed well with the calculated loss (3.9%). The residual compounds were amorphous.

Elemental analysis gave ratios Ti/P, F/P and N/P respectively of 0.85, 1.99 and 1.0 for phase **1** and 0.93, 2.01 and 0.98 for phase **2** (theoretical values for both phases: 1, 2 and 1). Moreover, the density measurements, performed on a Micromeretics Accupyc 1330 apparatus, were 2.46(2) g cm^{-3} for **1** and 2.36(1) g cm^{-3} for **2**, which agreed very well with the theoretical values: 2.47 and 2.35 g cm^{-3}.

Finally, these analyses corroborated the formulae deduced from the structures: $TiPO_4F_2^{-}{\cdot}0.5N_2C_2H_{10}^{2+}$ for **1** and $TiPO_4F_2^{-}{\cdot}0.5N_2C_3H_{12}^{2+}{\cdot}0.5H_2O$ for **2**.

2.2 Structure determinations

No single crystals of acceptable size could be obtained, even with very long synthesis times. Therefore, an *ab initio* structure

Table 1 Indexed powder pattern of $Ti_2(PO_4)_2F_4 \cdot N_2C_2H_{10}$ **1**[a]

h	k	l	d_{calc}/Å	d_{obs}/Å	Intensity	h	k	l	d_{calc}/Å	d_{obs}/Å	Intensity
1	0	0	7.1712	7.1723	100	0	4	0	2.2204	2.2204	1L
1	0	1	6.1632	6.1661	1L	1	4	0	2.1210	2.1213	1
−1	1	1	5.2613	5.2630	2	3	2	0	2.1048	2.1045	1L
0	2	0	4.4407	4.4438	1	3	1	1	2.0839	2.0845	1L
−1	0	2	4.2739	4.2697	6	0	3	3	2.0544	2.0547	1
0	1	2	3.8555	3.8557	1	−2	3	3	1.9732	1.9725	1
−1	2	0	3.7755	3.7768	1L	0	2	4	1.9278	1.9273	1L
2	0	0	3.5856	3.5897	6	−3	0	4	1.8979	1.8989	1L
−2	1	1	3.4337	3.4338	2	2	3	2	1.8730	1.8726	1L
−2	0	2	3.2653	3.2651	1	3	0	2	1.8651	1.8653	1L
0	2	2	3.0816	3.0809	26	1	1	4	1.8559	1.8602	1L
2	1	1	2.8467	2.8467	1L	−4	1	1	1.8292	1.8287	1L
0	3	1	2.7979	2.7981	1L	4	0	0	1.7928	1.7947	1L
−2	2	0	2.7897	2.7887	1L	−1	1	5	1.7538	1.7541	1L
0	1	3	2.7165	2.7156	1L	3	2	2	1.7196	1.7192	1L
−1	3	1	2.6964	2.6961	1L	0	1	5	1.6810	1.6808	1L
1	2	2	2.6348	2.6351	2	4	2	0	1.6624	1.6623	1L
−2	1	3	2.5366	2.5359	1L	2	3	3	1.6383	1.6390	1L
−3	1	1	2.4084	2.4065	1L	−3	4	2	1.6339	1.6343	1L
3	0	0	2.3904	2.3918	2	3	3	2	1.5780	1.5779	1
1	1	3	2.3319	2.3314	1L	1	1	5	1.5402	1.5405	1
−2	3	1	2.3172	2.3166	1L	−1	3	5	1.5312	1.5316	1L
−1	0	4	2.2403	2.2401	1						

[a] Indexing is based on a monoclinic cell with dimensions $a = 7.508(1)$, $b = 8.881(1)$, $c = 8.961(1)$ Å, $\beta = 107.22(1)°$. The symbol L refers to an intensity $\ll 1$.

determination from powder data was necessary. The powder diffraction diagrams were collected on a D5000 Siemens diffractometer; the XRD patterns of both compounds showed a strong preferred orientation effect due to their layered structure. Therefore, to minimise these effects, the powders were pulverised with a 'Mac Crone' grinder in ethanol (Prolabo, 95%) and dried at 373 K; the fine powders were introduced vertically in a 'Mac Murdie' type sample-holder. This led to a significant reduction of the preferred orientation effect, which remained however high, despite preferential orientation correction parameters used during the refinement.

The patterns were indexed with the Dicvol91 program.[22] Solutions in monoclinic systems were found with satisfactory figures of merit (M_{20}, $F_{20} = 21$, 26 for **1** and 23, 41 for **2**). The cell parameters could also be found from the complete data set by means of the NBS*AIDS83 program[23] [M_{20}, $F_{20} = 33$, 41 for **1** (0.01, 45) and 41, 53 for **2** (0.01, 46)]. Systematic absences were consistent with space group $P2_1/c$ (no. 14) for **1** and $C2$ (no. 2) for **2**. The indexed powder patterns are reported in Tables 1 and 2.

The pattern matching was performed with Fullprof 97,[24] and the structures were solved by direct method using Sirpow92.[25] During the refinements, which also used Fullprof, distance constraints were applied with mean distances Ti–X = 2 Å (X = O, F), P–O = 1.55 Å, N–C = C–C = 1.5 Å. Moreover, angular constraints for the organic templates used distance constraints between non-consecutive atoms $\{d[A(i)–A(i+2)] = 2.35$ Å$\}$. Because of its asymmetry and its strong preferred orientation, the first (and strongest) reflection was excluded, for each pattern, to improve the refinement. For compound **1**, the presence of aluminium reflections of the sample-holder on the pattern obliged us to exclude the area

Table 2 Indexed powder pattern of $Ti_2(PO_4)_2F_4 \cdot N_2C_3H_{12} \cdot H_2O$ **2**[a]

h	k	l	d_{calc}/Å	d_{obs}/Å	Intensity	h	k	l	d_{calc}/Å	d_{obs}/Å	Intensity
2	0	0	8.0507	8.0517	100	−5	1	2	2.4186	2.4179	1
0	0	1	6.0605	6.0685	1	5	1	1	2.3687	2.3696	1L
1	1	1	5.8948	5.9011	2	−2	2	2	2.2344	2.2338	3
−2	0	1	5.6986	5.6962	1	0	2	2	2.1895	2.1890	1
−1	1	1	4.4688	4.4711	6	7	1	0	2.1621	2.1611	1
2	0	1	4.2829	4.2838	2	1	3	0	2.0936	2.0931	1
−3	1	0	4.0929	4.0936	5	−4	0	3	2.0603	2.0601	1
4	0	0	4.0254	4.0259	19	0	0	3	2.0202	2.0198	1
−4	0	1	3.9157	3.9169	2	8	0	0	2.0127	2.0125	2
−3	1	1	3.8050	3.8004	1L	−1	3	1	2.0022	2.0014	2
0	2	0	3.1673	3.1654	10	−3	1	3	1.9948	1.9943	1
−2	0	2	3.1526	3.1545	8	−1	1	3	1.9763	1.9758	1
3	1	1	3.0912	3.0919	1	−3	3	0	1.9649	1.9662	1
0	0	2	3.0302	3.0298	6	−6	2	2	1.9025	1.9011	1L
2	2	0	2.9474	2.9469	7	7	1	1	1.8809	1.8808	1
−5	1	1	2.8998	2.8987	1	2	0	3	1.8379	1.8378	1L
−5	1	0	2.8706	2.8675	1	−9	1	1	1.7926	1.7932	1
−4	0	2	2.8493	2.8497	1	−5	3	0	1.7658	1.7659	1
−6	0	1	2.7681	2.7675	1	−7	1	3	1.7292	1.7299	1L
−3	1	2	2.7425	2.7426	1L	0	2	3	1.7032	1.7013	1L
6	0	0	2.6836	2.6838	2	1	3	2	1.6929	1.6935	1
2	0	2	2.5989	2.6003	1L	3	1	3	1.6712	1.6683	1L
−4	2	0	2.4891	2.4899	1L	4	0	3	1.6267	1.6263	1L
−4	2	1	2.4625	2.4634	1L	10	0	0	1.6101	1.6101	1

[a] Indexing is based on a monoclinic cell with dimensions $a = 16.821(2)$, $b = 6.335(1)$, $c = 6.331(1)$ Å, $\beta = 106.82(1)°$.

close to the strongest reflection ($2\theta = 36.5$–$38.5°$) of aluminium. Details of the structure refinements are summarised in Table 3.

The final agreement factors are $R_p = 16.2\%$, $R_{wp} = 21.6\%$ for **1** and $R_p = 20.9\%$, $R_{wp} = 26.3\%$ for **2**; because of the strong preferred orientation due to the morphology of the compounds, we could not obtain satisfactory refinements, particularly for compound **2**. Pattern matching of the refined structure of phase **1** is shown in Fig. 1. Atomic coordinates are summarised in Tables 4 and 5; bond distances and angles are given in Tables 6 and 7.

Table 3 Physical and crystal data for $Ti_2(PO_4)_2F_4{\cdot}N_2C_2H_{10}$ **1** and $Ti_2(PO_4)_2F_4{\cdot}N_2C_3H_{12}{\cdot}H_2O$ **2**

Formula weight	212	228
D_c/g cm^{-3}	2.47	2.35
Crystal system	Monoclinic	Monoclinic
Space group	$P2_1/c$ (no. 14)	$C2$ (no. 5)
Z	2	2
a/Å	7.508(1)	16.821(2)
b/Å	8.881(2)	6.335(1)
c/Å	8.961(1)	6.331(1)
β/°	107.22(1)	106.82(1)
V/Å^3	570.8(1)	645.8(1)
Radiation [λ(Cu)/Å]: Kα_1, α_2	1.54059, 1.54439	1.54059, 1.54439
2θ range/°	5–40; 40–80	8.50, 80
Step times/s	30; 60	120
Step size/°	0.02	0.02
Excluded regions (2θ)/°	5–13, 36.5–38.0	8.50–13.0
Total no. reflections	698	457
No. profile points	3751	3576
No. parameters refined	43	49
No. atoms refined	10	12
R_p (%)	16.2	20.9
R_{wp} (%)	21.6	26.3
R_{Bragg} (%)	12.0	18.4
R_F (%)	7.7	16.1

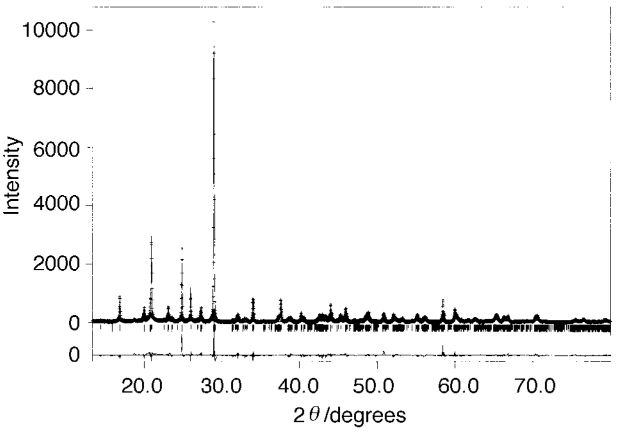

Fig. 1 Final Rietveld plot of $Ti_2(PO_4)_2F_4{\cdot}N_2C_2H_{10}$ **1**.

Table 4 Atomic coordinates ($\times 10^4$) of $Ti_2(PO_4)_2F_4{\cdot}N_2C_2H_{10}$ **1**

Atom	x	y	z
Ti	1188(6)	3(10)	2852(8)
P	165(16)	2490(10)	5050(22)
F1	−1218(16)	137(20)	2298(20)
F2	3882(15)	−240(17)	3363(17)
O1	1130(30)	−1510(25)	4433(26)
O2	1038(32)	1440(22)	1140(22)
O3	1240(30)	1515(25)	4383(25)
O4	847(28)	−1615(23)	1310(25)
N	5000(28)	1622(18)	1258(27)
C	5635(31)	650(21)	285(30)

Table 5 Atomic coordinates ($\times 10^4$) of $Ti_2(PO_4)_2F_4{\cdot}N_2C_3H_{12}{\cdot}H_2O$ **2**

Atom	x	y	z
Ti	−2145(9)	1042(33)	2832(12)
P	−2375(11)	5883(41)	2480(21)
F1	−3370(18)	645(53)	2242(30)
F2	−925(16)	1293(53)	3652(28)
O1	−1980(21)	3992(42)	3127(46)
O2	−2062(16)	1192(64)	−305(35)
O3	−2007(16)	1130(76)	6085(33)
O4	−2022(23)	−1860(43)	3095(45)
N	−305(19)	−1400(41)	8163(36)
C1	0000	−1190(60)	5000
C2	105(28)	−2760(43)	6910(32)
Ow	0000	−5130(55)	0000

Table 6 Interatomic distances (Å) and angles (°) for $Ti_2(PO_4)_2F_4{\cdot}N_2C_2H_{10}$ **1**

Ti–F(1)	1.73(1)	Ti–O(2)	1.97(2)
Ti–F(2)	1.95(1)	Ti–O(3)	1.91(2)
Ti–O(1)	1.96(2)	Ti–O(4)	1.96(2)
P–O(1)	1.48(3)	P–O(3)	1.43(3)
P–O(2)	1.38(2)	P–O(4)	1.47(3)
N–C	1.41(3)	C–C	1.49(3)
N–F(1)	3.02(3)	N–F(2)	2.82(2), 2.90(2)
F(1)–Ti–F(2)	176(1)	F(2)–Ti–O(4)	90(1)
F(1)–Ti–O(1)	91(1)	O(1)–Ti–O(2)	175(2)
F(1)–Ti–O(2)	85(1)	O(1)–Ti–O(3)	88(2)
F(1)–Ti–O(3)	87(1)	O(1)–Ti–O(4)	89(2)
F(1)–Ti–O(4)	87(1)	O(2)–Ti–O(3)	95(2)
F(2)–Ti–O(1)	90(1)	O(2)–Ti–O(4)	88(1)
F(2)–Ti–O(2)	94(1)	O(3)–Ti–O(4)	173(2)
F(2)–Ti–O(3)	96(1)		
O(1)–P–O(2)	114(3)	O(2)–P–O(3)	120(3)
O(1)–P–O(3)	106(3)	O(2)–P–O(4)	104(2)
O(1)–P–O(4)	111(3)	O(3)–P–O(4)	101(1)
P–O(1)–Ti	142(2)	P–O(3)–Ti	146(2)
P–O(2)–Ti	154(2)	P–O(4)–Ti	156(2)
N–C–C	113(3)		

Table 7 Interatomic distances (Å) and angles (°) for $Ti_2(PO_4)_2F_4{\cdot}N_2C_3H_{12}{\cdot}H_2O$ **2**

Ti–F(1)	2.00(3)	Ti–O(2)	2.03(2)
Ti–F(2)	1.95(3)	Ti–O(3)	2.00(2)
Ti–O(1)	1.89(3)	Ti–O(4)	1.85(3)
P–O(1)	1.37(4)	P–O(3)	1.57(3)
P–O(2)	1.44(3)	P–O(4)	1.55(4)
N–C(2)	1.47(5)	C(1)–C(2)	1.5(3)
N–F(1)	2.86(2)	N–F(2)	3.14(3), 3.23(3)
Ow–N	2.57(4)	Ow–F(1)	2.73(3)
F(1)–Ti–F(2)	175(3)	F(2)–Ti–O(4)	89(2)
F(1)–Ti–O(1)	105(2)	O(1)–Ti–O(2)	90(2)
F(1)–Ti–O(2)	101(2)	O(1)–Ti–O(3)	84(2)
F(1)–Ti–O(3)	90(1)	O(1)–Ti–O(4)	164(3)
F(1)–Ti–O(4)	89(2)	O(2)–Ti–O(3)	169(2)
F(2)–Ti–O(1)	77(2)	O(2)–Ti–O(4)	95(2)
F(2)–Ti–O(2)	84(2)	O(3)–Ti–O(4)	88(2)
F(2)–Ti–O(3)	86(2)		
O(1)–P–O(2)	122(4)	O(2)–P–O(3)	100(2)
O(1)–P–O(3)	105(4)	O(2)–P–O(4)	102(3)
O(1)–P–O(4)	127(3)	O(3)–P–O(4)	92(3)
P–O(1)–Ti	142(3)	P–O(3)–Ti	134(2)
P–O(2)–Ti	136(2)	P–O(4)–Ti	150(3)
N–C(2)–C(1)	95(2)	C(2)–C(1)–C(2)	99(2)

3 Discussion

These structures are two different monoclinic distortions of the layered oxovanadium(V) orthophosphate dihydrate $VOPO_4{\cdot}2H_2O$ **I** synthesised by Tietze.[26] The structure of $VOPO_4{\cdot}2H_2O$ exhibits tetragonal symmetry: space group $P4/nmm$ (no. 14) with $a = 6.202(1)$, $c = 7.410(1)$ Å and $V = 285.0(1)$ Å^3. The inorganic layers are made of an infinite array of PO_4 tetrahedra linked to VO_6 octahedra by sharing the oxygen atoms (Fig. 2). The vanadium is hexacoordinated but the octahedra are distorted because of a very short and a very long V–O distance due to the V=O and the V–H_2O bonding. These bonds are terminal and point perpendicularly to the inorganic layer; the other water molecule is located inside the interlayer space. The hydrogen bonds between this water molecule and the inorganic framework ensure the stability of the structure (Fig. 3).

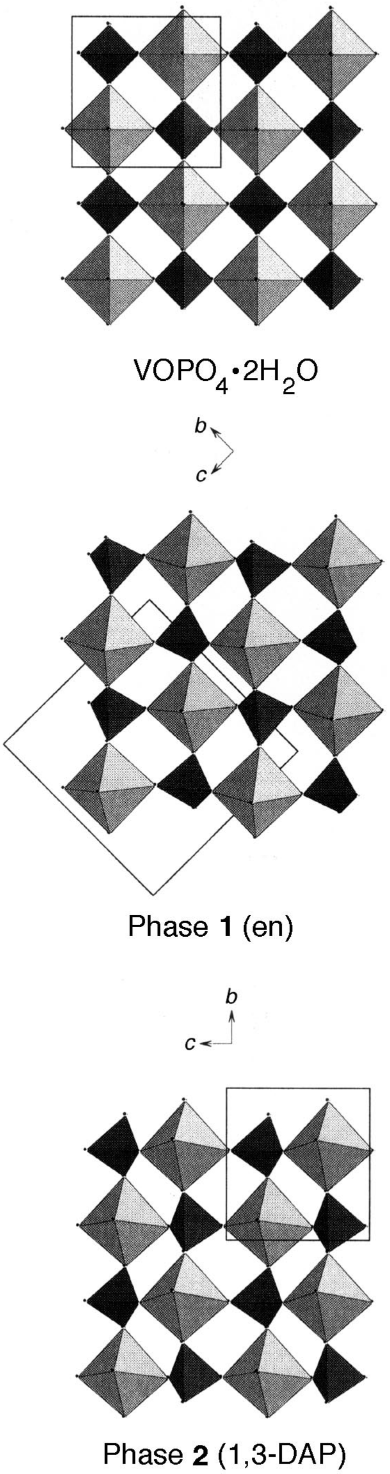
$VOPO_4 \cdot 2H_2O$

Phase **1** (en)

Phase **2** (1,3-DAP)

Fig. 2 View of the inorganic layers.

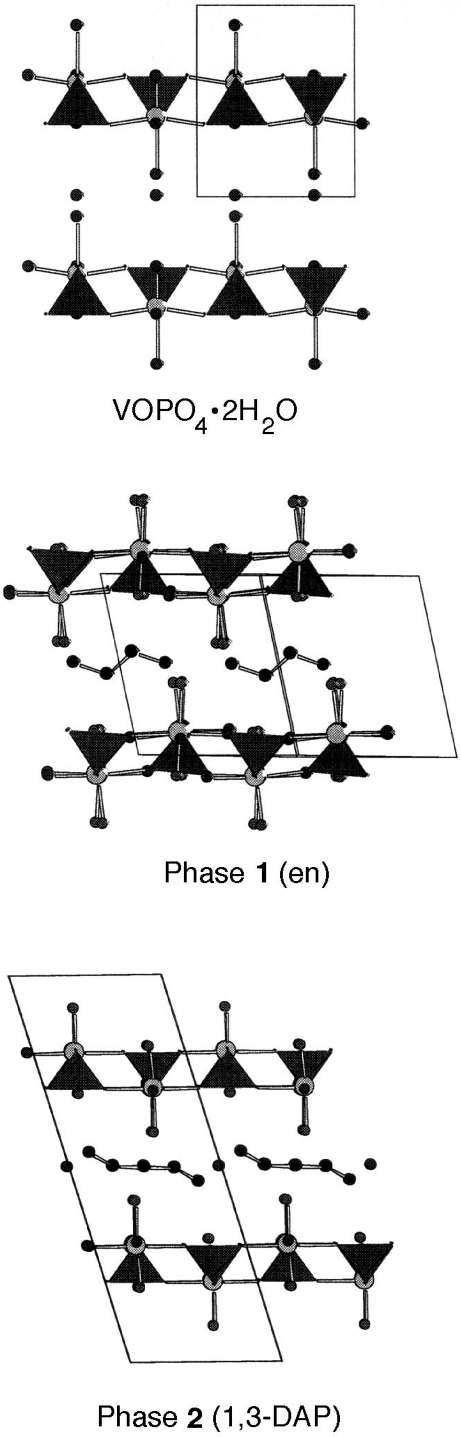
$VOPO_4 \cdot 2H_2O$

Phase **1** (en)

Phase **2** (1,3-DAP)

Fig. 3 View of the interlayer spacings.

In our case, the monoclinic symmetry comes from the length of the organic template which introduces geometrical constraints and lowers the symmetry. Metric relations are obvious between the three structures: $b(\mathbf{1})/\sqrt{2} \approx c(\mathbf{1})/\sqrt{2} \approx b(\mathbf{2}) \approx c(\mathbf{2}) \approx a(\mathbf{I})$ in the layer and $c(\mathbf{1})\sin\beta(\mathbf{1}) \approx c(\mathbf{2})/2 \sin\beta(\mathbf{2}) \approx c(\mathbf{I})$. Compared to the interlayer of the vanadium compound (7.41 Å), the difference of interlayer spacing between compounds **1** and **2** (7.17 and 8.08 Å respectively) mainly results from the positions of the terminal atoms on each structure (Fig. 3). In **2**, the terminal fluorine atoms, which point perpendicularly to the inorganic layer, are in front of each other and this increases the interlayer spacing, while in **1** the terminal fluorine atoms are shifted; the interlayer spacing of **1** is thus lower.

The respective locations of the fluorine and oxygen atoms was deduced from crystal chemistry considerations. While the large influence of preferred orientation prevents any distinction between oxygen and fluorine from the data, the four equatorial anions of the titanium octahedra, connected to PO_4 tetrahedra, must be oxygen atoms. Furthermore, chemical analysis showed a O/F ratio of 2/1; thus the two terminal anions of the titanium octahedra must be fluorine atoms.

Topologically, the inorganic layers of the vanadium and titanium compounds are very similar (Fig. 2 and 3): the V–H_2O and the V=O bonds are replaced by Ti–F bonds and the water molecule of the vanadium structure is replaced by the organic template in **1** and by a water molecule and the diamine in **2**. In both cases, strong hydrogen bonds, between the diprotonated ammonium heads and the fluorine atoms, ensure the stability of the structure.

Owing to the refinement from powder data, the interatomic distances and angles are only in broad agreement with those usually reported for titanium phosphates except for P–O distances which are found to be too short: 1.39–1.58 Å *cf.* 1.55 Å. Ti–F distances, almost equal in **2**, show a strong disparity in **1** (1.73 and 1.95 Å); the latter, related to the position of the amines, will be discussed below; these distances are quite long for Ti–F distances which are usually about 1.71 Å for terminal fluorine (mean distance reported in the crystal structure of TiF_4).[27]

Compounds **1** and **2** differ also by the location of the amines within the interlayer spacing (Fig. 4): the diamines of **1** are oriented perpendicularly to each other while in **2**, the organic species are in the same direction with ammonium groups in *cis* position which explains the non-centrosymmetry of the structure. Moreover, such a location of this amine in **2** leaves enough room for a water molecule (Fig. 4). The strong hydrogen bonds between this water molecule, amino groups and the inorganic framework [d(Ow–N) = 2.47 Å and d(Ow-F1) = 2.73 Å] is however in agreement with the existence of a monohydrate of 1,3-diaminopropane in the structure (Fig. 4 and 5). This association as already been encountered in ULM-3,[6] but not at such an acidic pH (1 instead of 5). Finally, the different locations of the amines in both structures explain why in **1** the only strong interaction between amino groups and fluorine is with F2 (1.95 Å) so leading to a terminal character for F1 (1.75 Å), while in **2**, the ammonium heads interact with both F1 (1.975 Å) and F2 (2.00 Å) (Fig. 5).

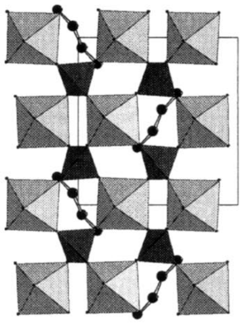

Phase **1** (en)

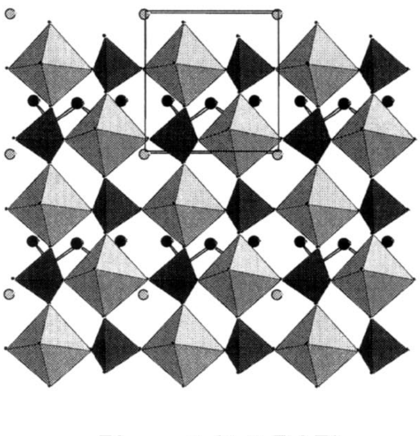

Phase **2** (1,3-DAP)

Fig. 4 Location of the organic template/layers.

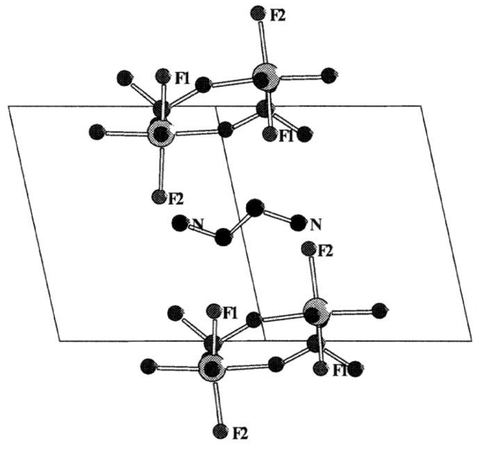

Phase **1** (en)

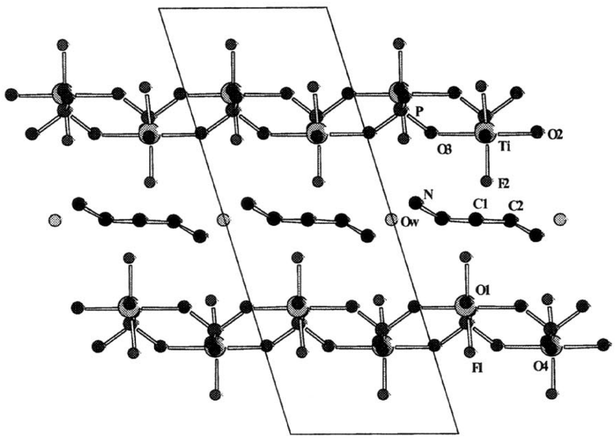

Phase **2** (1,3-DAP)

Fig. 5 Structural units of phases **1** and **2**.

These compounds are then two examples of different distortions occurring when the nature of the template is modified: from water in the vanadium structure to ethylenediamine and 1,3-diaminopropane (and water) in **1** and **2**. These compounds are the first oxyfluorinated titanium phosphates templated by organic templates; on the one hand, this opens a new way to the synthesis of titanium compounds and on the other, these results confirm the hypothesis of mechanism suggested by one of us,[1,2] stating that the nature of the metal is not the driving force for the synthesis of templated microporous compounds. Finally, several other phases, characterized subsequently show that the synthesis of microporous oxyfluorinated titanium phosphates is possible.

Acknowledgement

We gratefully acknowledge RHODIA for its financial support.

References

1 G. Férey, *J. Fluorine Chem.*, 1995, **72**, 187.
2 G. Férey, *C.R Acad. Sci.*, *Ser. IIc*, 1998, **1**, 1.

3 V. Soghomoniam, Q. Chen, R. C. Haushalter, J. Zubieta, C. J. O'Connor and Y. Lee, *Chem. Mater.*, 1993, **5**, 1690.
4 D. Riou and G. Férey, *Eur. J. Solid State Inorg. Chem.*, 1994, **31**, 25.
5 D. Riou and G. Férey, *J. Solid State Chem.*, 1994, **111**, 422.
6 M. Cavellec, D. Riou, J. M. Grenèche and G. Férey, *J. Magn. Mater.*, 1996, **163**, 173.
7 M. Cavellec, D. Riou, C. Ninclaus, J. M. Grenèche and G. Férey, *Zeolites*, 1996, **17**, 250.
8 M. Cavellec, J. M. Grenèche, D. Riou and G. Férey, *Microporous Mater.*, 1996, **8**, 103.
9 M. Cavellec, D. Riou, J. M. Grenèche and G. Férey, *Microporous Mesoporous Mater.*, 1996, **431**, 57.
10 M. Cavellec, D. Riou, J. M. Grenèche and G. Férey, *Microporous Mater.*, 1998, **8**, 103.
11 A. Clearfield and J. A. Stynes, *J. Inorg. Nucl. Chem.*, 1964, **26**, 117.
12 S. Allulli, C. Ferragina, A. La Ginestra, M. A. Massucci and N. Tomassini, *J. Inorg. Nucl. Chem.*, 1977, **39**, 1043.
13 R. Masse and J. C. Grenier, *Bull. Soc. Fr. Mineral. Cristallogr.*, 1971, **94**, 437.
14 R. Masse, A. Durif and J. C. Guitel, *Z. Kristallogr.*, 1974, **139**, 103.
15 C. Delmas and A. Nadiri, *Solid State Ionics*, 1988, **28–30**, 419.
16 Y. J. Li and M. S. Whittingham, *Solid State Ionics*, 1993, **63–65**, 391.
17 A. I. Bortun, L. N. Bortun, A. Clearfield, M. A. Villa-Garcia, J. R. Garcia and J. Rodriguez, *J. Mater. Res.*, 1996, **11**, 2490.
18 A. M. Krogh Andersen, P. Norby and T. Vogt, *Inorg. Chem.*, 1998, **37**, 4313.
19 D. M. Poojary, A. I. Bortun, L. N. Bortun and A. Clearfield, *J. Solid State Chem.*, 1997, **132**, 213.
20 M. B. Hursthouse, K. M. Malik, J. M. Thomas, J. Chen, J. Xu, T. Song and R. Xu, *Russ. Chem. Bull.*, 1994, **43**, 1787.
21 E. Kemnitz, M. Wloka, S. Trojanov and A. Stiewe, *Angew. Chem., Int. Ed. Engl.*, 1996, **35**, 2677.
22 Dicvol91, A. Boultif and D. Louer, *J. Appl. Crystallogr.*, 1991, **24**, 987.
23 A. D. Mighell, C. R. Hubbard and J. K. Stalick, Fortran program for crystallographic Data Evaluation, NBS (US Tech. Note 1141) (NBS*AIDS is an expanded version of NBS*AIDS80).
24 Fullprof, J. Rodriguez-Carvajal, in *Collected Abstracts of Powder Diffraction Meeting*, Toulouse, France, 1990, p. 127.
25 Sirpow, A. Altomare, M. C. Burla, M. Camalli, G. Cascarano, C. Giacovazzo, A. Guagliardi and G. Polidori, *J. Appl. Crystallogr.*, 1994, **27**, 435.
26 H. R. Tietze, *Aust. J. Chem.*, 1981, **34**, 2035.
27 H. Bialowons, M. Mueller and B. G. Mueller, *Z. Anorg. Allg. Chem.*, 1995, **621**, 1227.

Paper 8/02710B